# Interferometric wavefront sensors for high contrast imaging

**K. L. Baker**

*Lawrence Livermore National Laboratory, Livermore, CA, USA*
Baker7@llnl.gov

**Abstract:** Several novel interferometer configurations are presented which have a high signal-to-noise ratio making them suitable for high contrast imaging. High contrast imaging instruments, such as required to directly observe extrasolar planets, will require adaptive optics systems capable of reducing the atmospherically induced phase aberrations to a few nm of wave-front error. The interferometer designs presented are shown to provide a higher contrast and/or are more robust than the conventional Mach-Zehnder interferometer, which has previously been considered for high contrast imaging. In addition, all of the interferometric-based wave-front sensors are shown to provide a significant improvement in the achievable contrast ratio when compared with conventional adaptive optics systems containing Shack-Hartmann wave-front sensors.



**OCIS codes:** (010.1080) Adaptive optics; (010.7350) Wave-front sensing.

**References and Links**

1. K. L. Baker, E. A. Stappaerts, D. Gavel, S. C. Wilks, J. Tucker, D. A. Silva, J. Olsen, S. S. Olivier, P. E. Young, M. W. Kartz, L. M. Flath, P. Kruelevitch, J. Crawford and O. Azucena, "High-speed horizontal-path atmospheric turbulence correction using a large actuator-number MEMS spatial light modulator in an interferometric phase conjugation engine," Opt. Lett. **29** 1731 (2004).
2. J. R. P. Angel, "Ground-based imaging of extrasolar planets using adaptive optics," Nature **368**, 203 (1994).
3 Lisa A. Poyneer and Bruce Macintosh, "Spatially filtered wave-front sensor for high-order adaptive optics," J. Opt. Soc. Am. A **21** 810 (2004).
4 François Rigaut, Jean-Pierre Véran, and Olivier Lai, "An analytical model for Shack-Hartmann-based adaptive optics systems," SPIE **3353** 1038 (1998).
5 E. E. Bloemhof and J. K. Wallace, "Phase contrast wavefront sensing for adaptive optics," SPIE **5553** 159 (2004).
6 R. B. Blackman, *The Measurement of Power Spectra, From the Point of View of Communications Engineering*. (Dover, New York, 1959).
7 J. Millerd, J. Hayes, M. North-Morris, M. Novak and J. Wyant, "Pixelated Phase-Mask Dynamic Interferometer," SPIE **5531** 304 (2004).
8 Mahendra P. Kothiyal and Claude Delisle, "Shearing interferometer for phase shifting interferometry with polarization phase shifter," Appl. Opt. **24** 4439 (1985).
9 K. L. Baker and E. A. Stappaerts, "A single-shot pixellated phase-shifting interferometer utilizing a liquid-crystal spatial light modulator," Opt. Lett. **31** 733 (2006).
10 R.-C. Tyan, P.-C. Sun, A. Scherer and Y. Fainman, "Polarizing beam splitter based on the anisotropic spectral reflectivity characteristic of form-birefringent multilayer gratings," Opt. Lett. **21** 761 (1996).

## 1. Introduction

Interferometers which measure phase directly are the most widely used wave-front sensors for metrology applications, however, their use in fielded adaptive optics systems has been very limited [1]. There are several reasons for this including the fact that most AO systems utilize incoherent light and the self-referencing interferometers appropriate for temporally incoherent light are not well suited for self-bootstrapping operation under low light conditions. Interferometers do, however, have good signal-to-noise ratio (SNR) properties which give them an advantage for applications such as high contrast imaging. With this in mind we present several novel designs which are suitable for high contrast adaptive optics systems and are intended to be used in conjunction with a conventional AO system such as a Shack-

#74362 - $15.00 USD Received 24 August 2006; accepted 20 October 2006

Hartmann wave-front sensor. The conventional AO system would be used to bring the Strehl ratio high enough that a significant amount of the light passes through the "pinhole" of the interferometric sensor used to generate the reference wave.

## 2. Interferometer Designs

Interferometers have been considered previously for use in adaptive optics systems aimed at detecting extra-solar planets. One such interferometric system was proposed by J.R.P. Angel and represents a self-referencing interferometer in a Mach-Zehnder configuration [2]. This interferometer, with an anti-aliasing spatial filter modification [3,4], is shown below in Fig. 1(a). In this interferometer the two detectors collect interferograms with the reference beams out of phase by 180 degrees between the detectors. By phase stepping the reference beam by 90 degrees between two successive measurements, four 90 degree phase shifted channels can be obtained. Some of the drawbacks of this configuration include; non-common path errors between the signal and reference arms of the interferometer, the delay between the two arms must be actively maintained to within $\lambda^2/\Delta\lambda$, susceptibility to noise vibrations due to the separate paths and potential chromatic errors in the phase stepper [5], requires multilayer coatings. This design is also wasteful of the light in that it splits both the signal and core into both arms and then filters out the signal beam in one of the arms.

An improvement in the SNR of the Mach-Zehnder can be achieved by changing the configuration slightly. The changes, shown in Fig. 1(b), are such that all of the core/reference is sent through one arm and all of the signal beam through the other arm. By making this change, the SNR is increased by approximately the SQRT(2). This design still has essentially the same challenges and susceptibilities as the previous design but can achieve higher contrast.

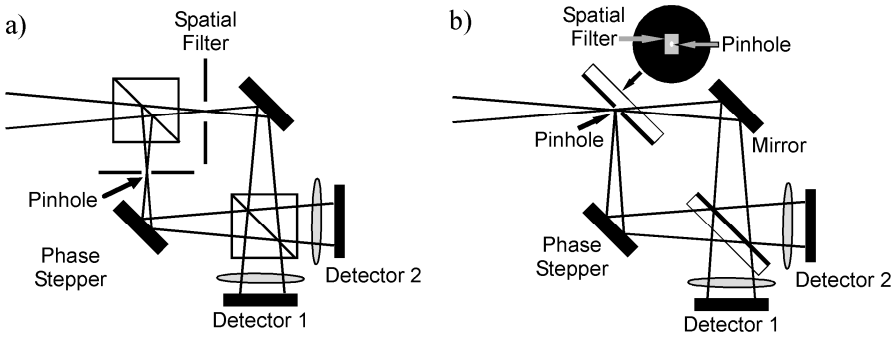


Fig. 1. Mach-Zehnder self-referencing wave-front sensor configurations. Fig 1a shows the design presented in Angel with a modification of a spatial filter to reduce aliasing and Fig 1b illustrates a design which incorporates the pinhole and spatial filter into the first beamsplitter, thereby improving the signal-to-ratio by a factor of the SQRT(2).

Wave-optics simulations of these two configurations were carried out to assess their achievable contrast. The "pinhole" in the first beamsplitter of the modified Mach-Zehnder was modeled with both a hard aperture and an apodized aperture as shown below in Fig. 2. The apodized aperture was modeled as an inverse Blackman apodizer with a transmission of unity in the center of the core tapering to zero at a radius of $\lambda/D$ [6]. This formed the reference wave and that function subtracted from 1 formed the reflected probe beam of the interferometer. By using the apodized filter, small values in the intensity of the probe beam were avoided as shown in Fig. 2 below. As such the apodized pinhole approach gave significantly better results and was chosen as the default configuration. This approach to pinhole apodization would be useful for all self-referencing interferometers and Zernike phase contrast [5] wave-front sensors which use a pinhole to separate both the reference and probe beams. The act of removing the core from the aberrated beam does change the behavior of the interferometer. In particular, the phase that is reconstructed has a multiplication factor associated with it, which for low Strehl ratio values is a function of the magnitude of the aberrations. At high Strehl

#74362 - $15.00 USD Received 24 August 2006; accepted 20 October 2006

ratio this multiplication factor is fairly constant and in the simulations performed for this article, the reconstructed phase was ~1.86 times the actual phase. In the case of the conventional Mach-Zehnder interferometer where the core is not removed from the signal beam, the reconstructed phase is equal to the actual phase.

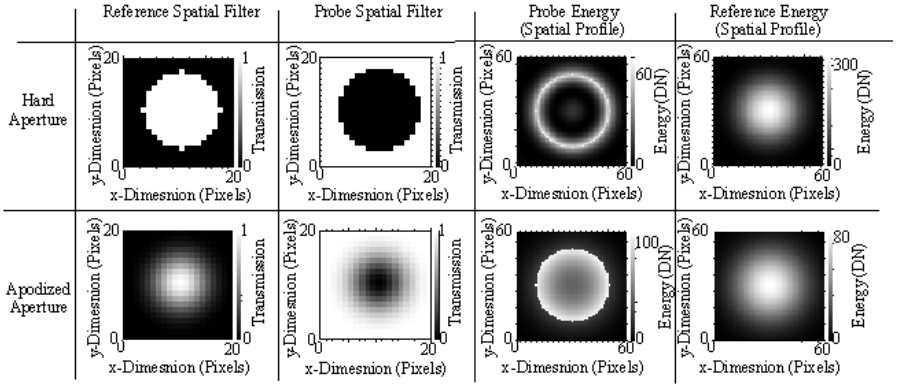


Fig. 2. Comparison between the spatial distribution of the probe and reference energy of the modified Mach-Zehnder interferometer when using a hard aperture, top, and an apodized beamsplitter, bottom inverse Blackman.

Recently a pixelated interferometer design [7] was developed based on the concept that left and right-hand circularly polarized beams develop a relative phase shift upon passing through a polarizer [8]. Wide bandwidth, >300 nm, wiregrid polarizers exist that transmit and reflect greater than 88% of the p and s polarized light, respectively, and narrow bandwidth thin film polarizers exist with less than 3 % absorption. A self-referencing version is shown below in Fig. 3. The unpolarized light is fist incident upon a polarizing plate, at 45 degrees, which splits the polarized beam between two symmetric arms of the wavefront sensor, one half of which is shown in Fig 3. The p polarized light passes through the polarizer and is then incident upon a polarization mask which has a vertically polarized circle, ~λ/D in diameter, at its center to provide a reference beam and horizontal polarization on the outer annulus which represents the signal beam. A square aperture placed on the horizontal polarization annulus provides spatial filtering to prevent aliasing. The achromatic quarter wave-plates create circularly polarized light and an array of polarizers placed on the detector provide the pixelated achromatic phase shifts between the beams. This design does not contain non-common path errors and hence is less susceptible to vibrations and phase stepping errors. It does incur a loss of >50% of the light due to the use of polarizers. This loss can be partially recovered by lower sampling of the pupil as discussed below.

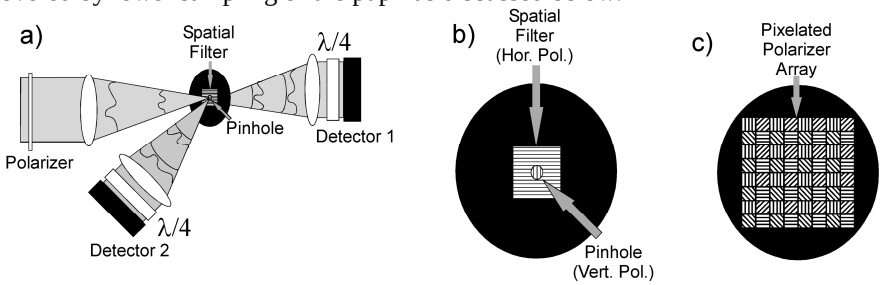


Fig. 3. Pixelated self-referencing wave-front sensor configuration, Figure 3a, with an enlarged image of the polarizing spatial filter/pinhole mask, Figure 3b, used to generate the spatially filtered signal waves and the reference waves and an enlarged picture of the pixilated polarizers, Figure 3c, in front of the detectors used to create the pixilated phase shifts. This image represents half of the interferometer with the identical remaining half taking the reflected light from the initial polarizer.

#74362 - $15.00 USD Received 24 August 2006; accepted 20 October 2006

A pixelated interferometer can also be made by creating an array of phase delays. This can be done using a pixelated deformable mirror(Liquid-crystal or MEMS), creating a phase array by etching a birefringent waveplate or building an array of multi-layer structures to provide the pixelated phase shifts [9]. In the case of broadband illumination, liquid-crystal spatial light modulators (LC-SLM) will have some dispersion associated with their use whereas the birefringent waveplate could in principle be made more achromatic. The advantage to this approach is that it could be implemented without the use of absorption polarizers which would increase its efficiency. The polarization spatial filter could be implemented from form-birefringent multilayer gratings [10] or thin films. A design for this type of pixelated wave-front sensor is shown below in Fig. 4. As in the previous design, the unpolarized light is first incident upon a polarizing plate, at 45 degrees, which splits the polarized beam between two symmetric arms of the wavefront sensor, one half of which is shown in Fig 4. The p polarized light passes through the polarizer and is then incident upon a polarization mask which has a vertically polarized circle, ~$\lambda$/D in diameter, at its center to provide a reference beam and horizontal polarization on the outer annulus which represents the signal beam. A square aperture placed on the horizontal polarization annulus provides spatial filtering to prevent aliasing. The reference beam and signal beams of orthogonal polarizations are sent through the same arm of the interferometer. The pixelated phase shift is accomplished by a birefringent array which could be an etched array from a conventional wave-plate [7] or a LC-SLM [9]. The pupil is imaged onto the phase delay array which is in turn imaged onto the detectors. Polarizing beamsplitters at 45 degrees to both the reference and probe beam polarizations are used to direct the signals to the four detectors. A much greater portion of the photons are used, making it more efficient that the design in Fig. 3, and only two detectors are required to measure the phase such that the redundant measurements can be averaged to reduce the noise. This interferometer is a common path design, except for the phase delay element, with the probe and reference passing through the same optics which reduces problems with vibrations and optics quality and removes the requirements to actively maintain the path length between the reference and probe beams as required by the Mach-Zehnders in Fig. 1.

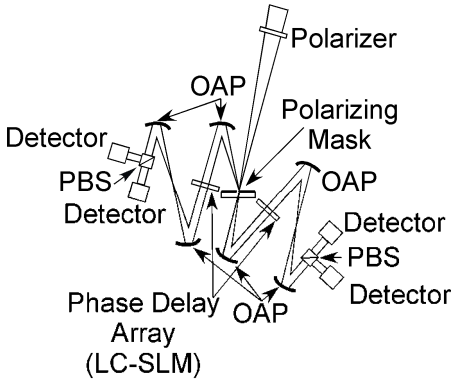


Fig. 4. A more efficient pixelated self-referencing wave-front sensor configuration that uses a LC-SLM: PBS's, polarizing beamsplitters; OAP, off-axis parabolas. The polarizing mask in this interferometer is the same as the one in Figure 3b. This image represents half of the interferometer with the identical remaining half taking the reflected light from the initial polarizer.

The phase shifting scheme for the pixelated self-referencing interferometer is shown in Fig. 5. In this case, the pixelated phase measurements between detector 1, Fig, 5(a), and detector 2, Fig. 5(b), are shifted relative to one another. The classic four phase shift interferometric wave-front sensor requires four CCD pixels/phase measurements per sub-aperture in the case of the Mach-Zehnder configuration. The pixelated interferometer has essentially two CCD pixels/phase measurements per sub-aperture in Fig. 5. In the case of the classic four phase shift interferometer, the phase is determined by using the reconstruction

#74362 - $15.00 USD Received 24 August 2006; accepted 20 October 2006

formula, $\mathrm{Tan}(\phi+\zeta)=(I_{3\pi/2}-I_{\pi/2})/(I_0-I_\pi)$, where the $I_{3\pi/2}$, $I_{\pi/2}$, $I_0$ and $I_\pi$ represent the measured intensities in the four CCD pixels. In the case of face centered reconstruction for the pixilated interferometer in Fig. 5(c), the reconstruction formula takes on the form

$$\mathrm{Phase}(i,j)=\mathrm{ATAN}\left\{\frac{I_{3\pi/2}(i,j)-0.25\left[I_{\pi/2}(i,j+1)+I_{\pi/2}(i,j-1)+I_{\pi/2}(i-1,j)+I_{\pi/2}(i+1,j)\right]}{I_0(i,j)-0.25\left[I_{\pi}(i,j+1)+I_{\pi}(i,j-1)+I_{\pi}(i-1,j)+I_{\pi}(i+1,j)\right]}\right\}. \quad (1$$

The intensities/phase steps are taken from a five pixel cross with the sub-aperture in the center of the cross as shown in Fig. 5(c). As it is readily apparent, even though there are only two phase shifts per subaperture, the phase can be reconstructed at a pitch equivalent to the subaperture pitch.

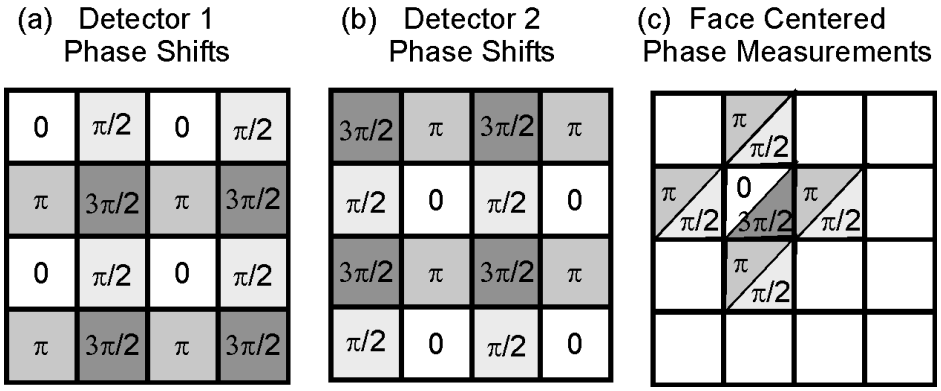


Fig. 5. Pixelated phase shifts and wave-front measurement grid.

### 3. Simulation Results with Atmospheric Turbulence

To measure the performance of the different sensors, simulations were performed with a fixed Kolmogorov phase screen with a Fried parameter of 0.3 m at 850 nm. The phase screen was spatially filtered to remove components that were beyond the Nyquist frequency of the deformable mirror. The phase screen was first operated on by a Shack-Hartmann (SH) wave-front sensor for five iterations to reduce the level of aberrations such that the interferometric wave-front sensors were operating in a non-phase-wrapped regime.(In the case of the SH sensor, 10 iterations were performed.) The interferometers ran for five iterations and the residual aberrations in the pupil were then apodized with a Blackman apodizer before being Fourier transformed to form the point spread function (PSF). A radial average of the PSF was taken and the result compared with the different configurations. For the simulations in Fig. 6 the electron read noise was 1 e- and the photons per subaperture was set at 225(corresponding to a G5 star at 30 pc in the I/Z band at 2 khz). Fig 6 shows a comparison between the Mach-Zehnders in Fig. 1(a) and Fig. 1(b), a Shack-Hartmann and the pixilated interferometers in Fig. 3 and Fig. 4. Figure 6(a) and 6(b) show the same data, however, Fig. 6b is zoomed in to show the differences between the interferometer performances. Even though there is a loss of 50 % of the photons due to the use of polarizers, the pixilated design in Fig. 3, dark gray line, can be implemented with two pixels per subaperture rather than four with a minimal loss in spatial resolution as discussed above and the interferometer makes better use of the photons it receives in a similar manner as the modified Mach-Zehnder. The modified Mach-Zehnder in Fig. 1(b), dashed black line, performs quantitatively better than the Mach-Zehnder in Fig. 1(a). The pixilated interferometer in Fig. 4, light gray line, which uses all of the photons provides an equivalent performance to the Mach-Zehnder in Fig. 1(a).

#74362 - $15.00 USD Received 24 August 2006; accepted 20 October 2006

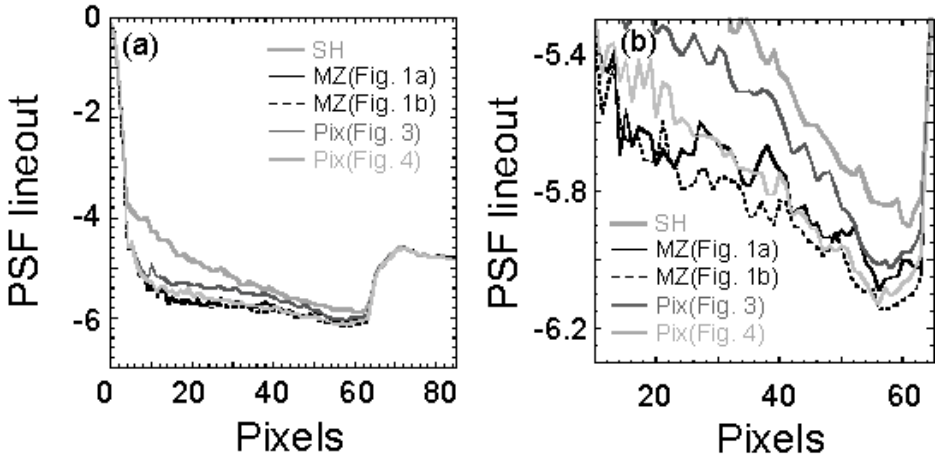


Fig. 6. Radially averaged PSF comparisons between the different interferometer and Shack-Hartmann configurations. Fig. 6a shows the radially averaged PSF over the entire range. Fig. 6(b) zooms in to make the differences in the interferometers more apparent.

## 4. Summary

In this article several novel interferometer designs were presented which had a higher SNR and/or were more robust than previous interferometric designs for high contrast adaptive optics. These designs included modifications to the standard Mach-Zehnder, as well as, pixelated designs. The effective spatial resolution of the pixelated designs was determined via simulations and their performance compared with the Mach-Zehnder. Finally a comparison was presented between the standard Mach-Zehnder and a Shack-Hartmann wave-front sensor showing the improvement in contrast that can be achieved with interferometric wave-front sensors. The modified Mach-Zehnder design was shown to provide the best performance overall with all of the interferometric designs providing higher contrast than the Shack-Hartmann wave-front sensor.


## Acknowledgments

The author would like to acknowledge many useful discussions with B.A. Macintosh, D.W. Phillion, L.A. Poyneer and B.J. Bauman. This work was performed under the auspices of the U.S. Department of Energy by the University of California, Lawrence Livermore National Laboratory under contract No. W-7405-Eng-48.


#74362 - $15.00 USD Received 24 August 2006; accepted 20 October 2006